X-613-66-190

NASA TM X- 55488

SOME RESULTS CONCERNING THE PRINCIPAL AIRGLOW LINES AS MEASURED FROM THE OGO-II SATELLITE

BY
EDITH I. REED
JACQUES E. BLAMONT

GPO PRICE $ _____

CFSTI PRICE(S) $ _____

Hard copy (HC) 2.00

Microfiche (MF) .50

APRIL 1966 ff 653 July 65

GODDARD SPACE FLIGHT CENTER
GREENBELT, MARYLAND

Corrected May 1966

SOME RESULTS CONCERNING THE PRINCIPAL AIRGLOW LINES AS MEASURED FROM THE OGO-II SATELLITE

by

Edith I. Reed
Goddard Space Flight Center
National Aeronautics and Space Administration
Greenbelt, Maryland

and

Jacques E. Blamont
Centre National de la Recherche Scientifique
Paris, France

ABSTRACT

Two photometers on the OGO-II spacecraft (launched October 14, 1965, 420 km perigee, 1520 km apogee, 87.4° inclination) scanned the airglow horizon through a filter centered at 6300A, the nadir airglow at 6300A, 6225A, 5890A, 5577A, 3914A, and 2630A, and the zenith airglow at 6300A. During its less than 10 days of stabilized operation approximately an hour of data were obtained while in the earth's shadow. The nadir measurements observed the blue enhancement at twilight, several aurorae, and typical nighttime airglow. The horizon scanning photometer observed the two airglow layers, a thick one generally above 200 km attributed to the 6300A line of atomic oxygen and a thin layer centered between 75 and 105 km attributed to the OH emissions which fall within the 40A wide passband of the interference filter. The maximum emission of the 6300A line occured generally between 200 and 300 km altitude with values of 1 to 25 photons cm^{-3} sec^{-1} at night and about a factor of 10 greater in the twilight.

SOME RESULTS CONCERNING THE PRINCIPAL AIRGLOW LINES AS MEASURED FROM THE OGO-II SATELLITE

by

Edith I. Reed
Goddard Space Flight Center
National Aeronautics and Space Administration
Greenbelt, Maryland

and

Jacques E. Blamont
Centre National de la Recherche Scientifique
Paris, France

INTRODUCTION

Airglow features seem to be on a very large scale, hundreds or thousands of kilometers in extent. Clusters of observatories along with airplane flights have revealed some of these features. There have been few observations in relatively inaccessible areas such as the polar regions and over the oceans. But these have merely intensified the desire for a better picture of the world-wide distribution of the airglow and its variations. Furthermore, many wavelengths of the airglow emissions are absorbed by the lower atmosphere and simply cannot be observed from the ground.

Another area in which ground observations are difficult is that of determining the altitude distribution of the emissions. The features are too poorly defined for use of simple triangulation techniques, yet the layers are far enough from being uniform that the van Rhijn method using the intensity as a function of zenith angle must make use of a large number

of scans (e.g. see Kulkarni). Rocket-borne instruments have given us reliable measurements of the vertical distribution of many of the airglow emissions below 200 km (Packer, Tarasova and Slepova). But only recently have 6300A photometers been flown to altitudes appreciably above this (Nagata).

It was to obtain information in these three areas, the large scale distribution of the principal emission lines, to study the ultraviolet emission in the vicinity of 2600A, and to measure the vertical distribution of the 6300A emission, that instrumentation was proposed for the Polar Orbiting Geophysical Observatory.

INSTRUMENTATION

Two photometers are used. Their locations on the spacecraft are shown in Figure 1. The Polar Orbiting Geophysical Observatory (POGO) is a box with one side facing the earth, with solar paddles which move to face the sun, and with an Orbital Plane Experiment Package (OPEP) which moves so that one of its faces is always perpendicular to the direction of motion. One of the photometers is located in the Main body, and can observe both the earth and the sky in six different wavelengths. The second is located in the OPEP and contains a moving mirror to enable it to scan across the earth's horizon ahead of the spacecraft. This photometer is sensitive only to the 6300A emission.

Schematics of the optical paths for the Main Body Photometer are given in Figures 2 and 3. This photometer uses only one photomultiplier with a tri-alkali cathode. Figure 2 shows the ray traces for a simple telescope in which the image of the objective lens is focussed upon the photocathode. So that we can use the same photomultiplier for measurement of both sky and earth, the path has been folded by insertion of two 45^{o} flats. This set of optics with a 5 cm diameter objective lens and a field of view of 4^{o} half angle is used to measure the 6300A light above the spacecraft. Figure 3 shows the optics used in the measurement of light below the spacecraft in six different wavelength regions. Here, again, light from a 5 cm diameter objective lens with a 5^{o} half angle field of view follows a folded optical path and is finally focussed on the photocathode.

By placing M_1 and M_2 on a common shaft, it is possible to direct the incoming light through any of six different filters. In a seventh position, Mirror M_2 is in the position of M_2 in Figure 2, and light from the up direction is directed to the photocathode. In the eighth and last position of the mirrors, the filter position is blanked off, and no light is directed to the photocathode. In regular operation the different wavelengths are measured in a fixed sequence, each of them being measured for one second every eight seconds. The wavelength and bandwidth of each filter is given in Table I. Every 200 seconds the shutters are

closed for 10 seconds and three small incandescent lamps located just inside the shutters and in the blanked-off sector are turned on to give a measure of the stability of the photometer. A cut-away drawing of this instrument is shown in Figure 4. Also shown are the electronic cards beneath the optical system, the position of iris-type shutters just in front of the objective lenses, and sliding doors to protect against contamination before and during launch. Photodiodes close the shutters in the presence of excessive light.

In Figure 5, an optical diagram of the OPEP photometer is given. Here again the optical path is folded to permit a compact, lightweight structure. The incoming light is reflected by a large (11.6 cm x 12.8 cm) moving mirror to a small Newtonian telescope which focusses the light on a slit. Near the slit is placed an interference filter peaked at 6291A with a bandwidth of 40A. The light passing through the slit falls on a tri-alkali cathode of a side window photomultiplier. The field of view as defined by the slit is $\frac{1^o}{2}$ in height and 6^o wide. By moving the entrance mirror the center of the field of view can be moved from horizontal to 30^o below horizontal in $\frac{1^o}{2}$ steps.

A cut-away view of the OPEP photometer is given in Figure 6. This view also shows the sliding door that protected the instrument during preparation and launch. In

orbit a small knife-like shutter was closed as needed to protect the photocathode from excessive light (as sensed by a photodiode) and also during a portion of the calibration sequence.

The time required for the OPEP photometer to scan across its 30^{o} field of view is 34.7 seconds, during which the spacecraft moves about 250km. As soon as one scan is complete the motion reverses direction and a new scan is started at the same rate. Every 200 seconds, the scanning motion is stopped, two small incandescent lamps are turned one, and the shutter closes during the eight second calibration cycle.

From the data describing the observed intensity as a function of angle, and assuming a number of thin uniform layers, the emission (photons cm^{-3} sec^{-1}) as a function of altitude can be computed. The center of the region thus described ranges from 1500 to 4500 km from the spacecraft, depending on both the altitudes of the spacecraft and of the region, but with 2000 km being representative for the data in this paper.

This spacecraft, known as OGO II, was placed in a nearly polar orbit (87.4^{o} inclination) October 14, 1965 with its apogee near 1500 km and its perigee near 400 km, and with a period of 104 minutes. It was soon noted that the attitude control system was using its supply of control gas far more rapidly than anticipated. Hence, for the next ten days, commands were given to the spacecraft so that there

were four periods of time totaling 52 hours during which the attitude of the spacecraft was such that one side faced the earth, the other the sky, and the solar paddles followed the sun. Since the photometers were not designed to protect themselves from excessive light under all conditions, they were turned off when the attitude was not stabilized.

During the times of stable attitude, the Main Body photometer was on for 38.7 hours, and the OPEP photometer for 32.6 hours. Because the spacecraft was launched at dawn so that it would be sunlit 100% of the time for its first few days of life, most of this data represents sunlit conditions of the earth's atmosphere. However, during the last two periods of stable operation, the plane of the orbit had changed sufficiently so that there were eclipse periods up to 11 minutes in length during which the spacecraft was in the earth's shadow. Of the time the spacecraft was stable, the Main Body photometer was on during the eclipse for a total of 2 hours and the OPEP photometer for a total of 1.6 hours. Data coverage was nearly fulltime since there are on-board tape recorders.

LATITUDE DISTRIBUTION OF AIRGLOW

The Main Body photometer was designed to make measurements in the earthward direction when the earth's surface was dark and the earthward side of the spacecraft was not illuminated by the sun, in other words, only when the spacecraft was

in the earth's shadow. The eclipse portions of the orbit during which data were obtained were centered at a latitude of about 37^{o}N and at most covered 36^{o} of latitude. Figure 7 is prepared from data obtained during one of the longer eclipses. The spacecraft was within a few degrees of its ideal position throughout this time. The moon was a thin crescent and was not visible from the surface of the earth.

The graph consists of straight lines drawn between each measurement. A measurement consists of an average of the data received during the one second that the light passes through a given filter, and is an average of the 2 or 3 read-outs obtained during that second. Instrumental corrections have been applied so that the amount of light entering the photometer is known within $\pm$ 50%. The total amount of light entering the photometer has been expressed in Rayleighs, with the assumption that the light is monochromatic at the stated wavelengths, except that for the 2630A data the emission is assumed to be uniform over the 205A passband of the filter. No attempt has been made to subtract light reflected from the earth and lower atmosphere (with a total albedo ranging between 15 and 65%, depending on wavelength, surface, and cloud cover).

It is apparent that the 5577A emission of atomic oxygen, the 5890A emission of sodium, and the emissions of OH near 6225A have a strong correlation with each other. The 6300A emission of atomic oxygen is relatively, but not completely independent.

As would be expected, there is little 6300A light above the spacecraft which is at altitudes between 420 and 470 km. The auroral emission of N_2^+ at 3914A is also weak, as is generally true at these latitudes. The filter centered at 6225A passes two lines of the OH emissions, and is also a measure of the OH emissions which are included in the 6300A signal. The emissions through the 2630A filter are barely detectable and their fluctuations are due principally to the noise of the photometer.

The high correlation between the 5577A emission of atomic oxygen and the sodium group of emissions (which includes the OH emissions) indicates that their fluctuations have a common cause. The magnitude of the variations is fairly consistent with the difference in albedo between open water and cloudy skies. However, the cell structure suggested by Roach and his colleagues cannot be ruled out.

In a pass a few hours later (125° longitude), these emissions had approximately the same ratio to each other, but the large scale variations were completely absent between 50 and 30 degrees latitude. A three to four-fold increase, resulting in a peak near 25 degrees latitude, is attributed to a large excursion in spacecraft attitude.

During a series of passes over the North Pole (orbits 105-109), the earthward shutter of the Main Body photometer remained open although the spacecraft was sunlit, and a series of latitude profiles across the auroral zone during the night were obtained. No auroral forms in the inner

auroral zone were apparent. These data will be further discussed later in this paper.

VERTICAL PROFILES

During the eclipse phase in all of the approximately 120 profiles computed from the OPEP photometer data, there are two maxima of intensity, one at 90 ± 15 km and the second around 240 km. Figure 8 shows an example of an observed horizon and Figure 9 the computed emission profile.

The observation of an emitting layer below 110 km is consistent with earlier rocket observations of red emissions detectable through a filter centered at 6300A (Heppner, Tarasova and Slepova). It is generally agreed that deactivation of the excited oxygen atoms by collision with molecules prevents the radiation of 6300A from atomic oxygen at these low altitudes. Its altitude is similar to that of the OH emissions observed in other wavelengths by various rocket-borne photometers (Packer). Its total intensity is generally less than 25 Rayleighs.

As far as the maximum around 240 km is concerned, it must be attributed to the [OI] 6300A emission. The shape of the maximum seems consistent with current theories attributing the emission to dissociative recombination (Lagos, Bellew, and Silverman; Lagos). The intensity of this peak during our experiments underwent a tendency to decrease when the latitude in the Northern Hemisphere would go from 50° to 20°, the only region where measurements are available. See Figure 10.

When the spacecraft was not in the earth's shadow, it was possible for light scattered from other portions of the spacecraft to enter the OPEP photometer, adding to and at times overwhelming the signal due to airglow or aurora. The interpretation of the data was further complicated by a modulation of the stray light by an oscillation of the OPEP container of $\pm 3^{o}$ about its ideal position of having its forward face perpendicular to the plane of the satellite's orbit. However, under some conditions it was possible to identify and subtract the contribution due to light scattered from the spacecraft, particularly when the earth beneath was not sunlit, as was true in the north polar region.

The maximum emission of the 6300A line in the night airglow varied from nearly 25 photons cm^{-3} sec^{-1} to less than 1 photon cm^{-3} sec^{-1}. Twilight maxima were typically between 20 and 50 photons cm^{-3} sec^{-1}.

AURORAL DATA

Between 0321 and 1347 GMT, October 22, 1965, data were obtained over part of the northern polar cap with both photometers. The geomagnetic planetary 3-hr. range index, K_p, ranged from 1 to 3+ during this time. Figure 11 shows the intensity of the 6300A emission recorded by the Main Body photometer as a function of geomagnetic latitude and geomagnetic time. Figure 12 shows the intensities at 3914A and 5577A recorded by the Main Body photometer in the same coordinate system. During two passes the auroral region was crossed twice, once in the late afternoon, then later during the

the same pass, just before dawn. A series of profiles were recorded during the same time by the OPEP photometer. In Figure 13 are two emission profiles, one shortly before sunrise and one shortly before sunset. These were computed using the same methods as earlier, with the assumption that the emission can be described as uniform horizontal layers. Hence, until the actual horizontal distribution of the aurora is taken into account, these altitudes must be taken only as lower limits for these aurora. Similarly the intensity may also include the effect of foreshortening. However, the study of several scans of each aurora indicates that the altitude of the maximum emission rate of the morning aurora is definitely lower than that for the evening.

Several tendencies can be noted: the 6300A [OI] emission is less intense and at somewhat lower altitudes in the early morning, and the location of the auroral emissions tends to be at higher geomagnetic latitudes in the late afternoon around 1700 hours geomagnetic time than in the early morning hours around 0400. This may be due in part to the fact that the aurora is sunlit at 1700 hours but not at 0400, but is also consistent with various theories and observations which indicate that the energy spectrum of auroral particles tends toward higher energies in the morning. The greater penetration of the particles produces the maximum [OI] 6300A emission at lower altitudes but of less intensity since a greater fraction of the excited atoms lose energy through molecular collisions.

CONCLUSION

During the short life of OGO-II as a properly stabilized Geophysical Observatory, some observations of the airglow and aurora were made, particularly in the northern hemisphere. The most significant part of the data is expected to be the vertical profiles of the [OI] 6300A emissions. When properly correlated with other types of observations a better understanding of the night, and possibly twilight airglow should result. The auroral data, when combined with possible ground observations should provide a more complete picture of an aurora than available heretofore.

ACKNOWLEDGEMENTS

The authors are indebted to the support received from our governments which enabled scientists and engineers from both laboratories to work together productively in all phases of this investigation. We also thank the many engineers and their colleagues at Goddard Space Flight Center for their skill in implementing the design of these photometers. Finally, we acknowledge the support given through the OGO Project Office at Goddard Space Flight Center in all facets of the preparation, launch and operation of the Observatory.

REFERENCES

1. J. P. Heppner and L.H. Meredith, Nightglow Emission Altitudes from Rocket Measurements, J. Geophys. Res. 63, No. 1 (March 1958) 51-65.
2. P. V. Kulkarni, On the Height of the 5577Å [OI] Airglow Layer in Hawaii, Annales de Géophysique 21, No. 1 (Jan-March 1965) 58-67.
3. P. Lagos, The Airglow 6300Å [OI] Emission, the Luminosity Profile with Varying Scale Height, J. Atmos. Terr. Phys. 26 (1964) 325-334.
4. P. Lagos, W. Bellew, and S. M. Silverman, The Airglow 6300Å [OI] Emission Theoretical Considerations on the Luminosity Profile, J. Atmos. Terr. Phys. 25 (1963) 581-587.
5. T. Nagata, T. Tohmatsu and T. Ogawa, Rocket Measurements of the 6300Å and 3914Å Dayglow Features, Planet. Space Sci. 13 (1965) 1273-1282.
6. D. M. Packer, Altitudes of the Night Airglow Radiations, Annales de Géophysique 17, No. 1 (1961) 67-75.
7. F. E. Roach, E. Tandberg-Hanssen and L. R. Megill, The Characteristic Size of Airglow Cells, J. Atmos. Terr. Phys. 13 (1958) 113-121.
8. T. M. Tarasova and V. A. Slepova, Altitude Distribution of the Radiation Intensity of the Main Emission Lines of the Night Sky, Geomagnetizm i Aeronomiia 4, No. 2 (March-April 1964) 321-327.

TABLE I

Direction of field of view	Center wavelength of filter	Effective bandwidth of filter
Down	2630 A	205 A
Down	3914 A	59 A
Down	5577 A	54 A
Down	5893 A	64 A
Down	6225 A	57 A
Down	6300 A	59 A
Up	6300 A	60 A

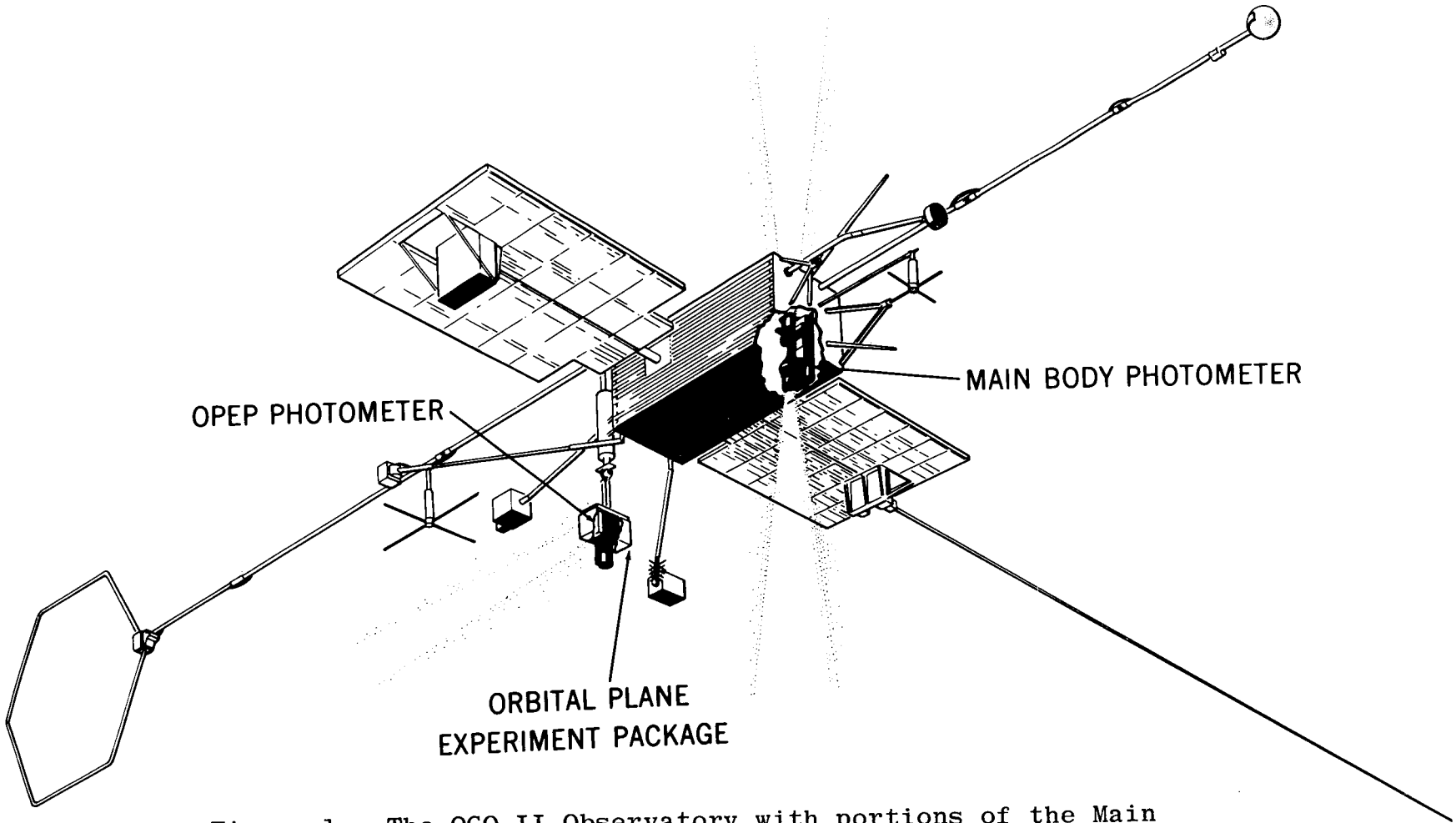

Figure 1. The OGO-II Observatory with portions of the Main Body and Orbital Plane Experiment Package cut away to show the two airglow photometers. The shading indicates the fields of view.

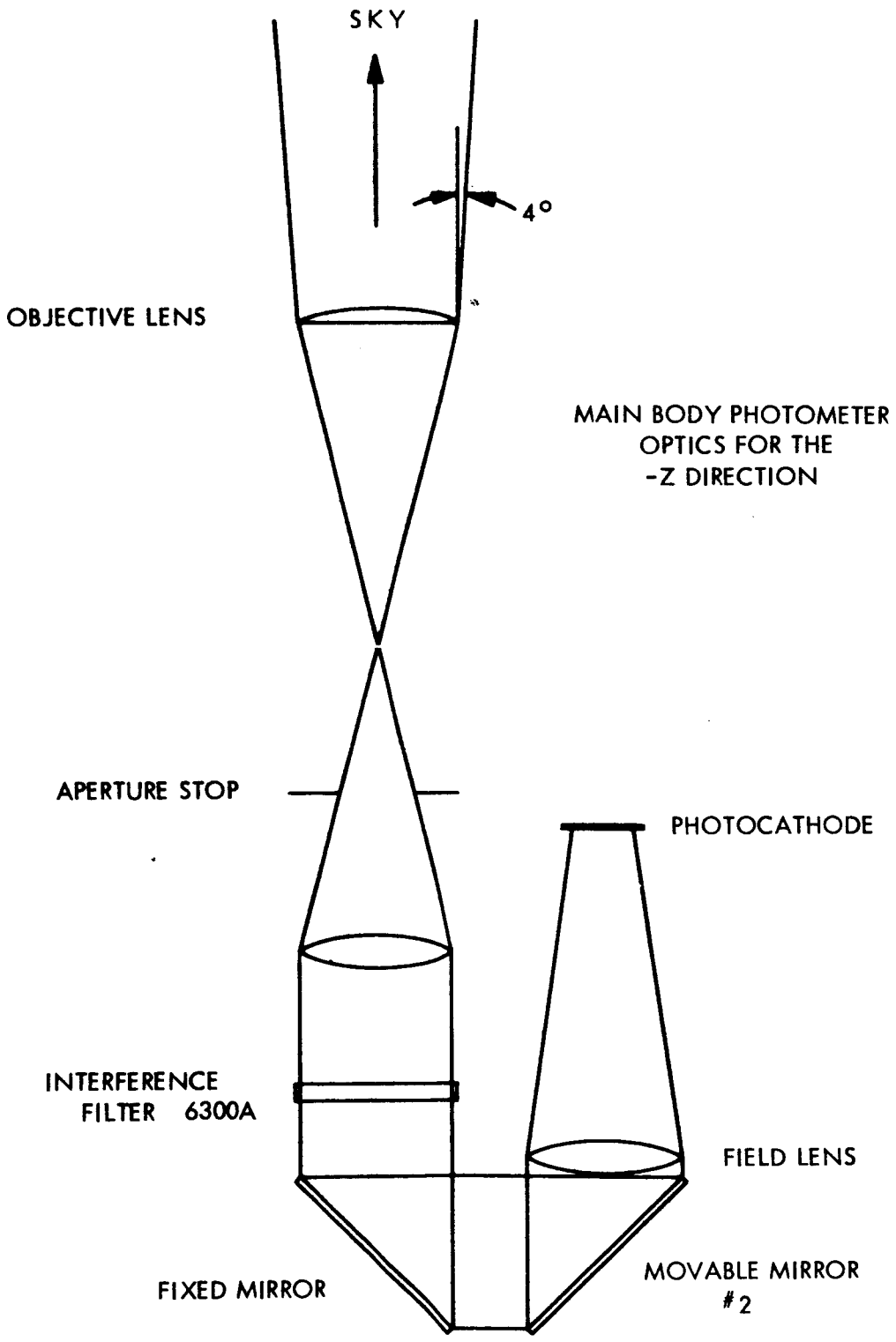

Figure 2. Ray traces for the optics used in making measurements towards the zenith.

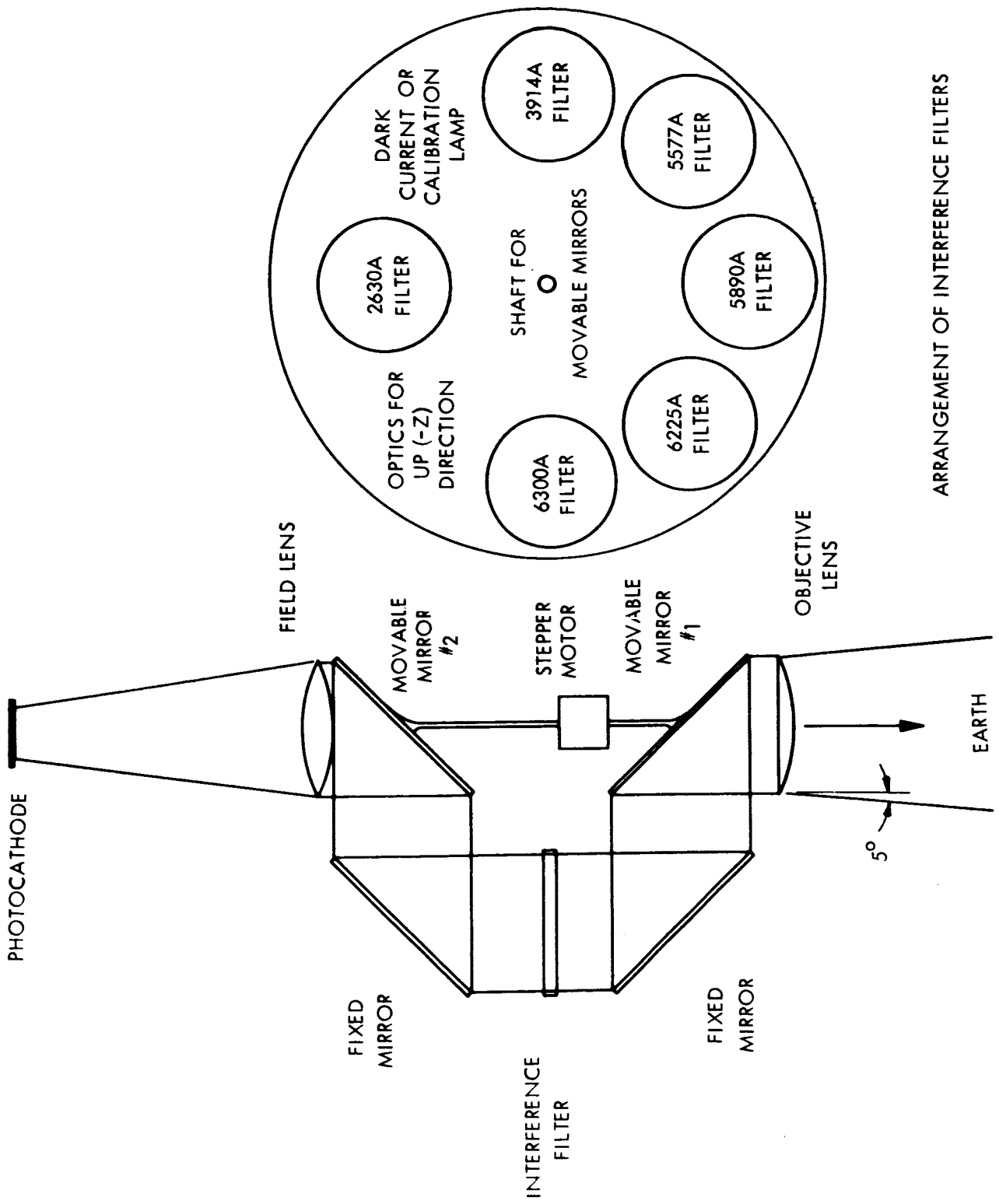

Figure 3. Ray traces for the optics used in making measurements towards the nadir. The filters and associated mirrors remain fixed in position while the two central mirrors direct the light to each filter in turn.

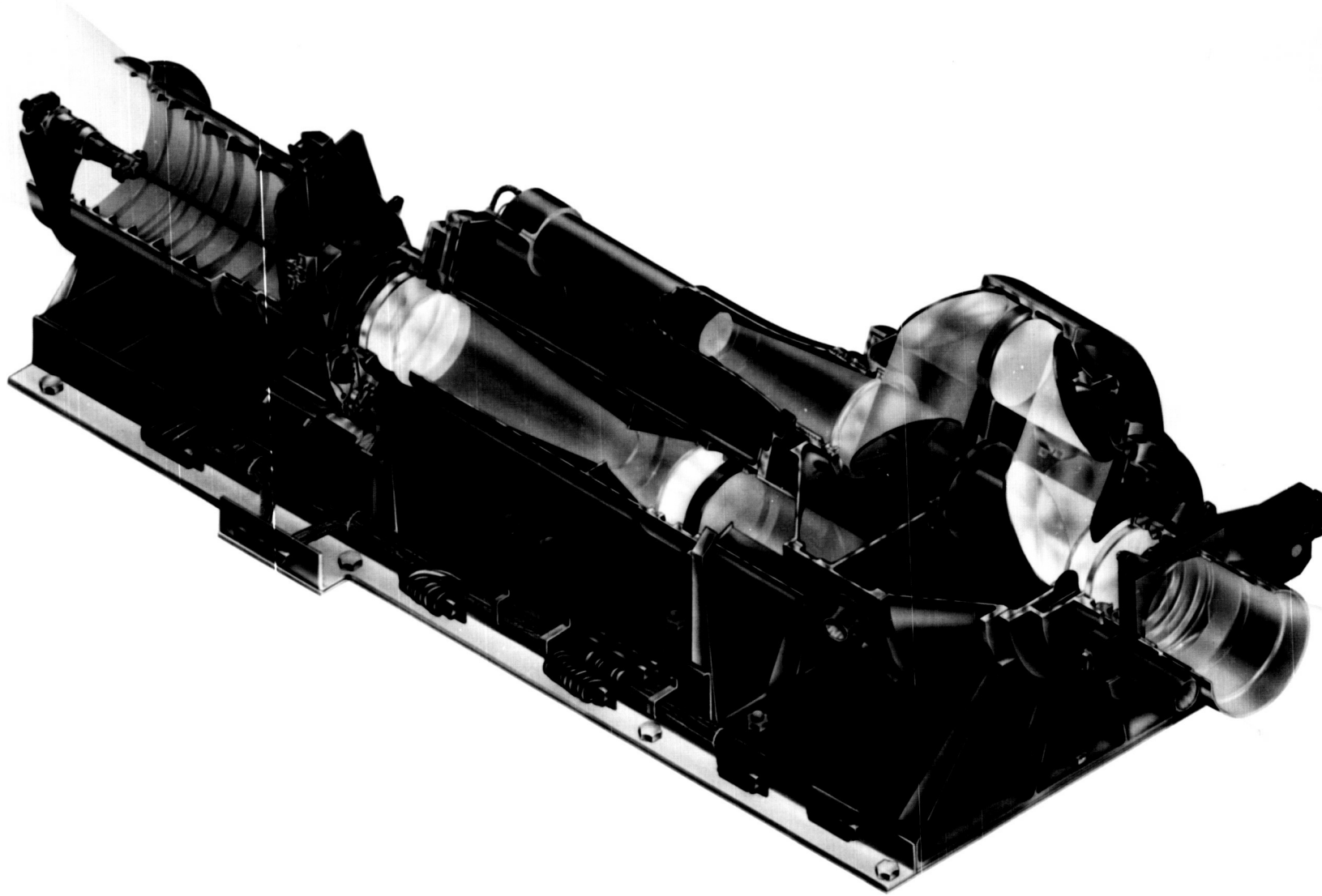

Figure 4. Main Body Photometer. A cut-away view with shading added to indicate the light paths.

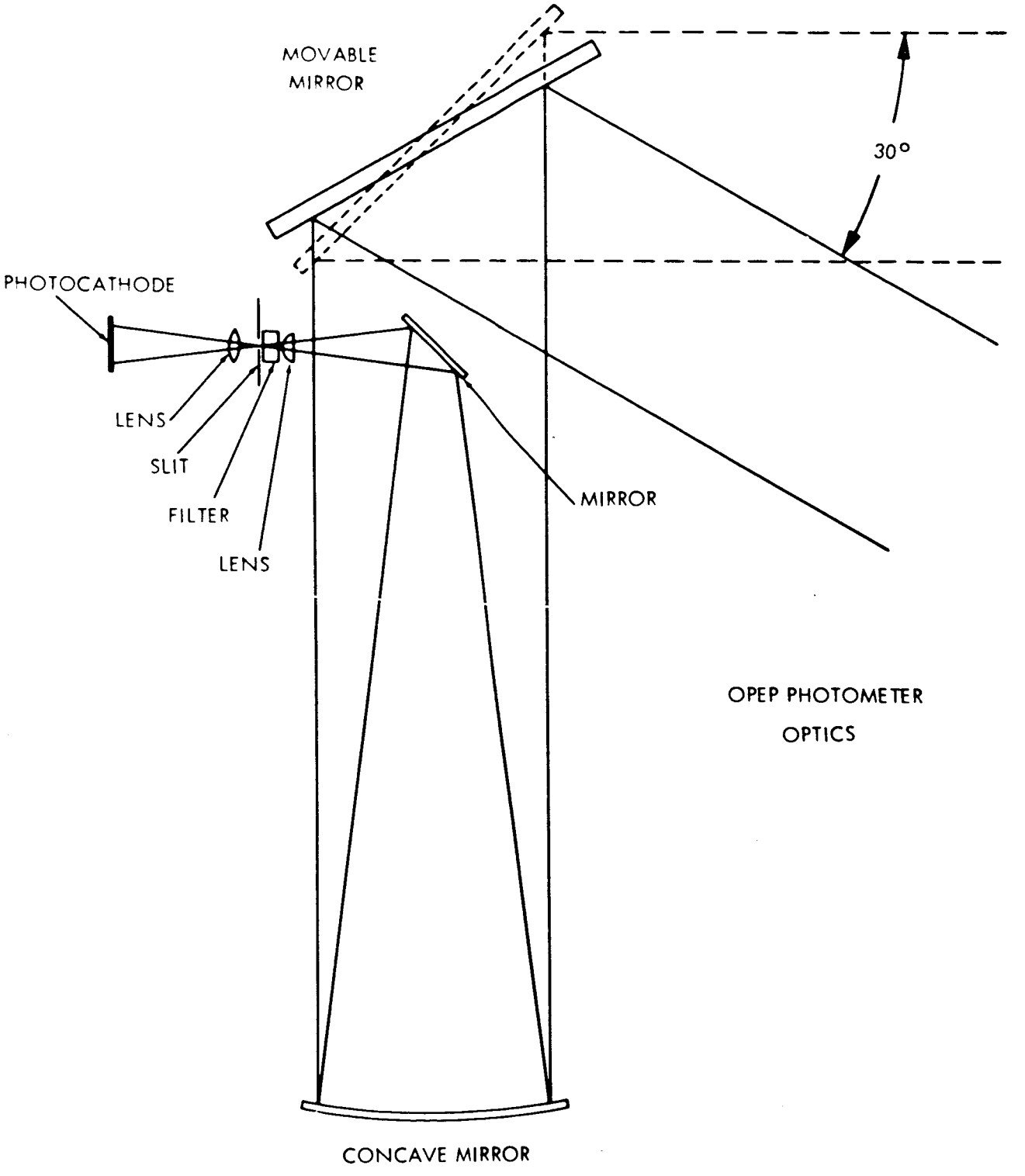

Figure 5. Ray traces for the optics for scanning across the horizon of the earth.

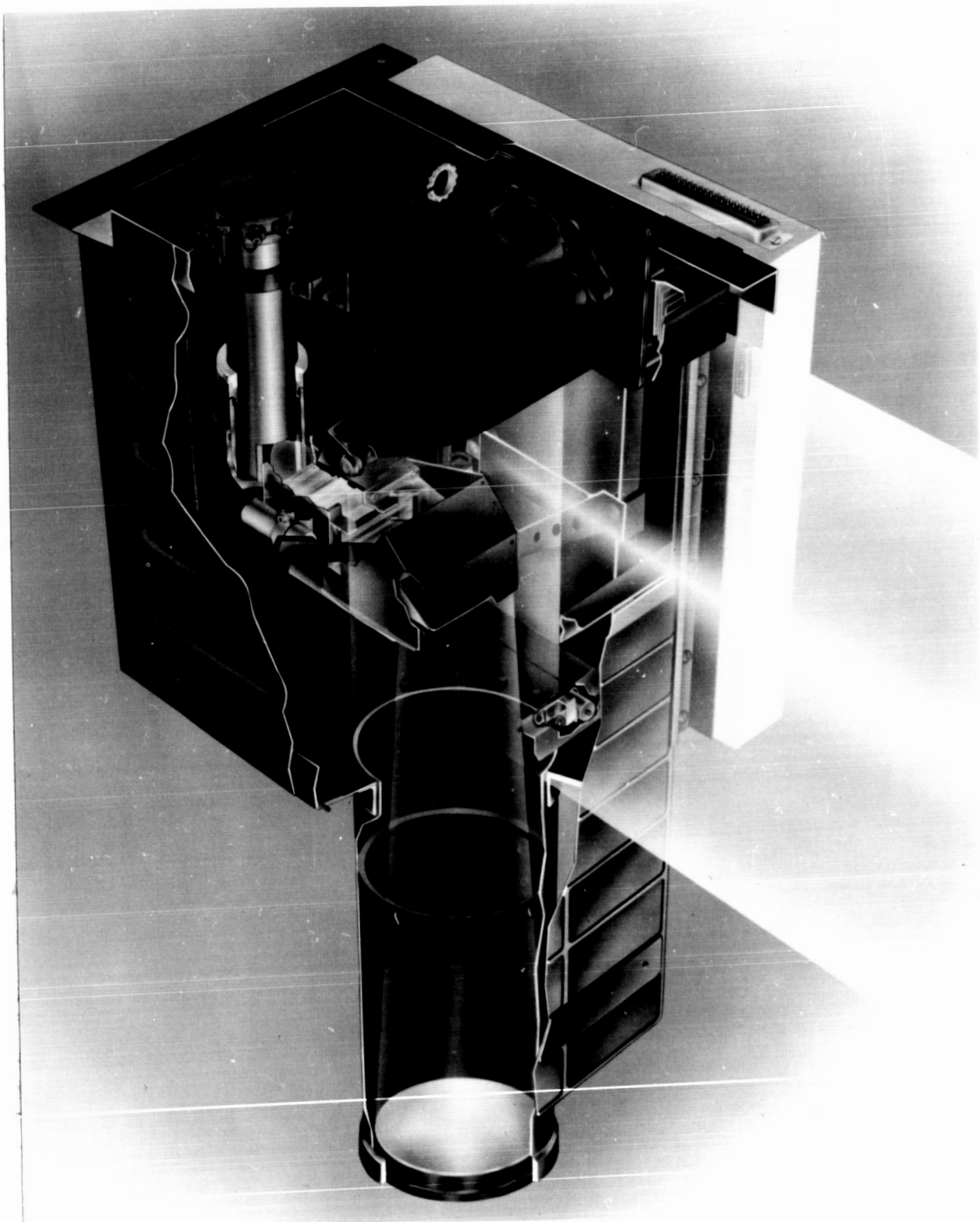

Figure 6. OPEP Photometer. A cut-away view with shading added to indicate the light path.

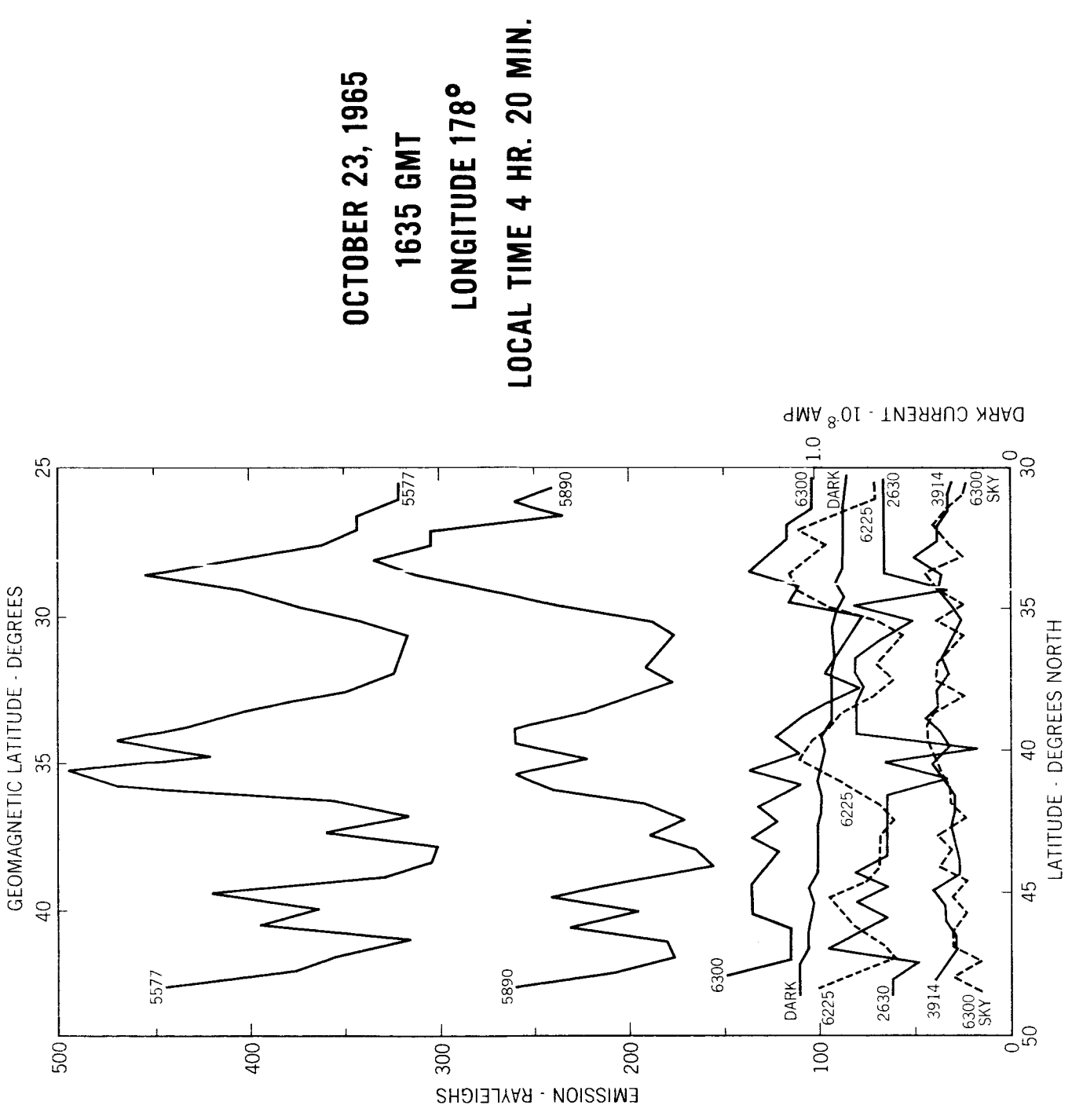

Figure 7. Observed intensities of light directly below the spacecraft. The conversion factors are about 400 Rayleighs per volt for the 2630 channel and between 50 and 200 Rayleighs per volt for all other channels.

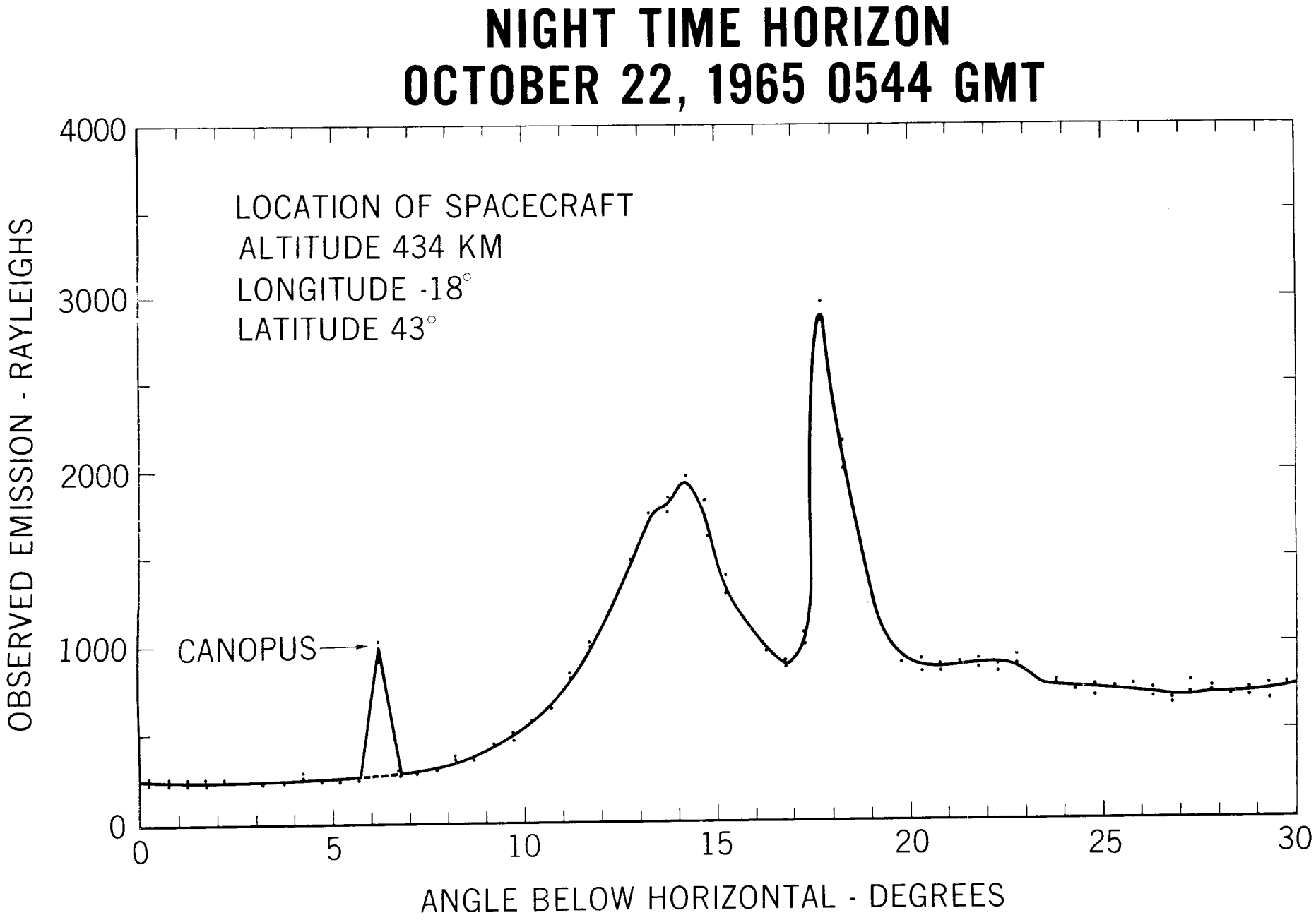

Figure 8. The observed brightness as a function of the angle below the horizontal plane of the spacecraft.

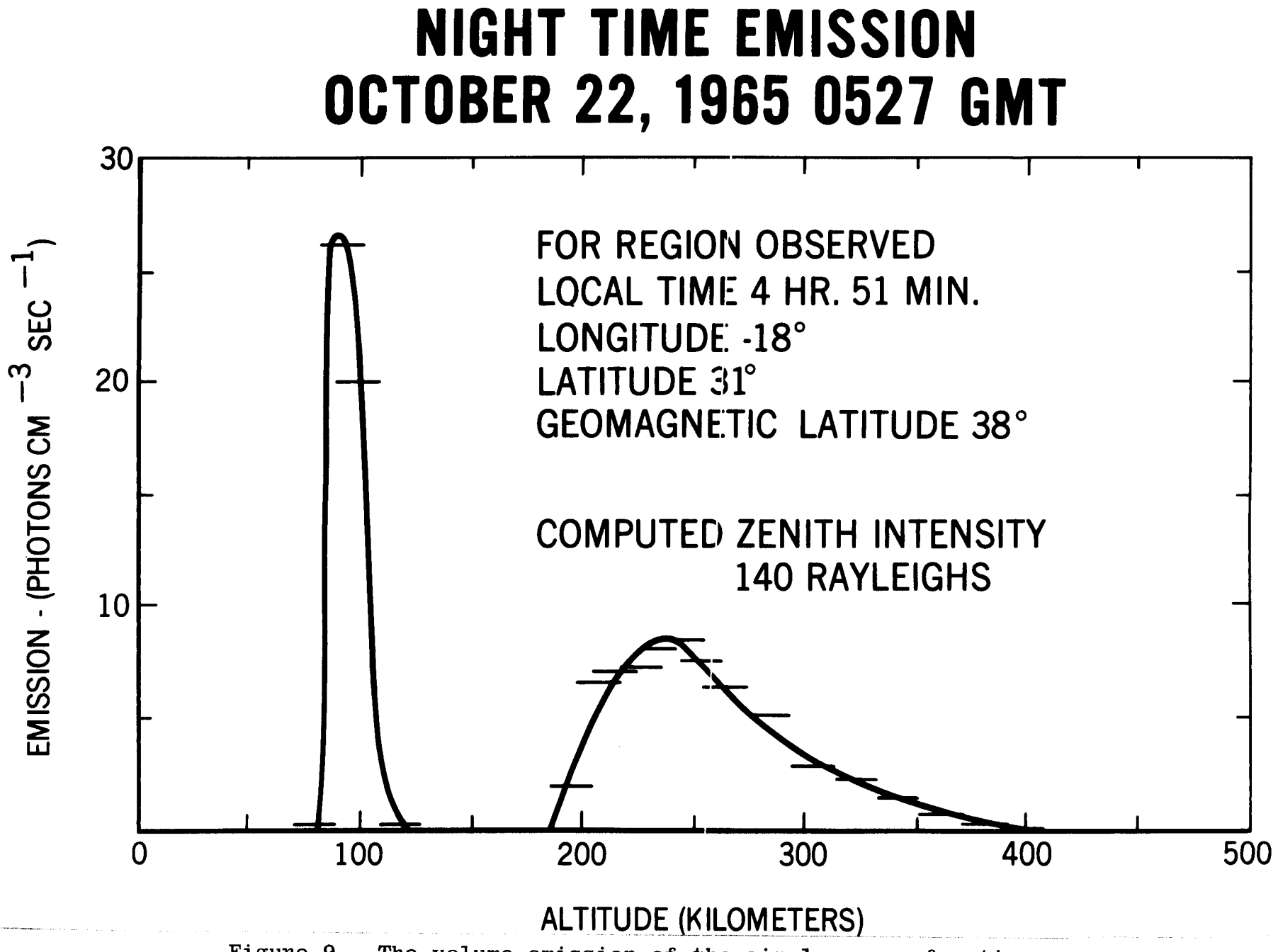

Figure 9. The volume emission of the airglow as a function of altitude, computed from the data of Figure 8.

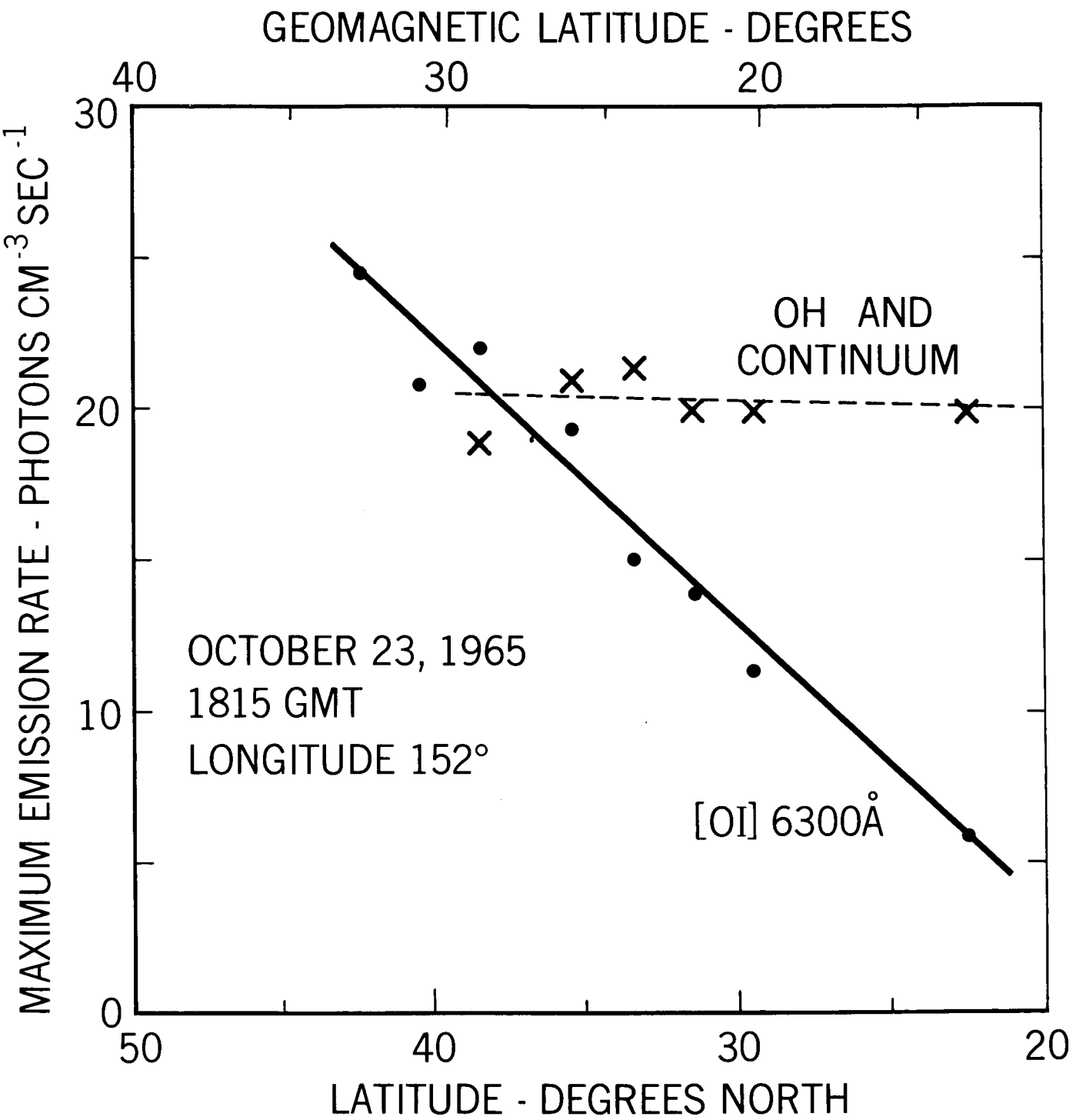

Figure 10. One of several series of observations of the emission profile as the spacecraft passed through the earth's shadow. In other passes the decrease in maximum emission rate was less marked.

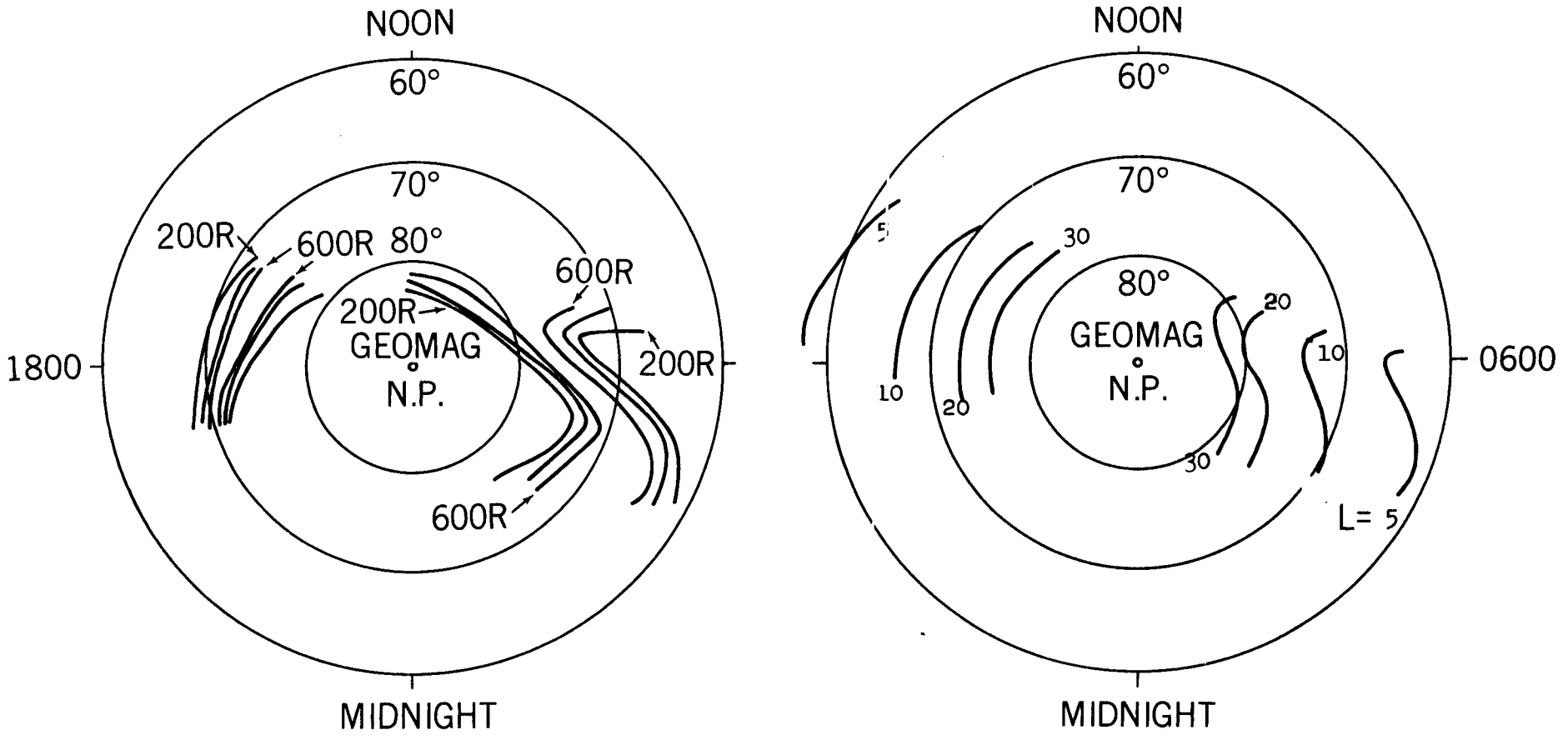

Figure 11. The brightness at nadir as the spacecraft passed over the auroral zone at altitudes between 400 and 700 km. For comparison the L-parameter values at the spacecraft are given.

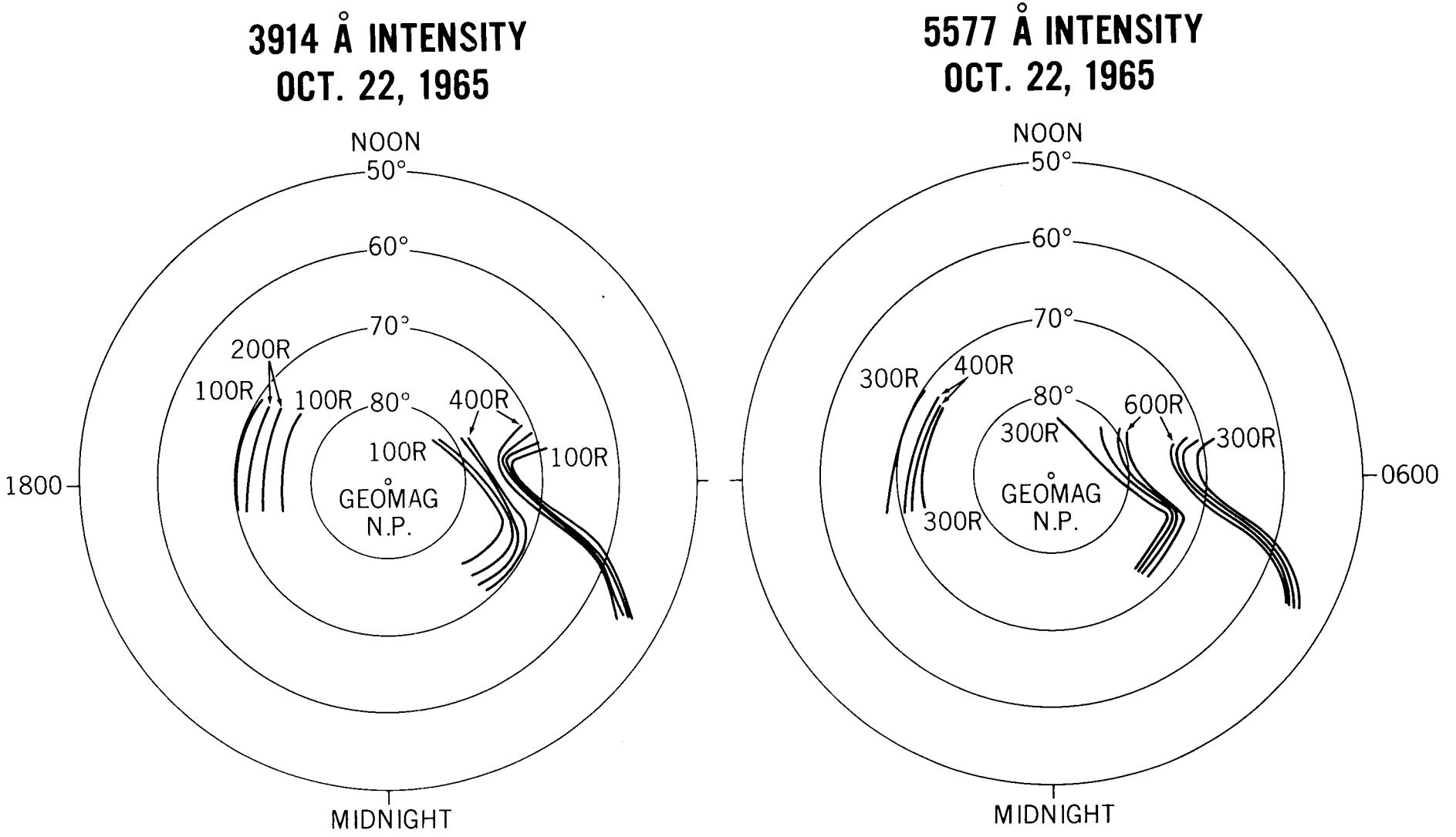

Figure 12. The brightness of other auroral emissions measured at the same time as that in Figure 11.

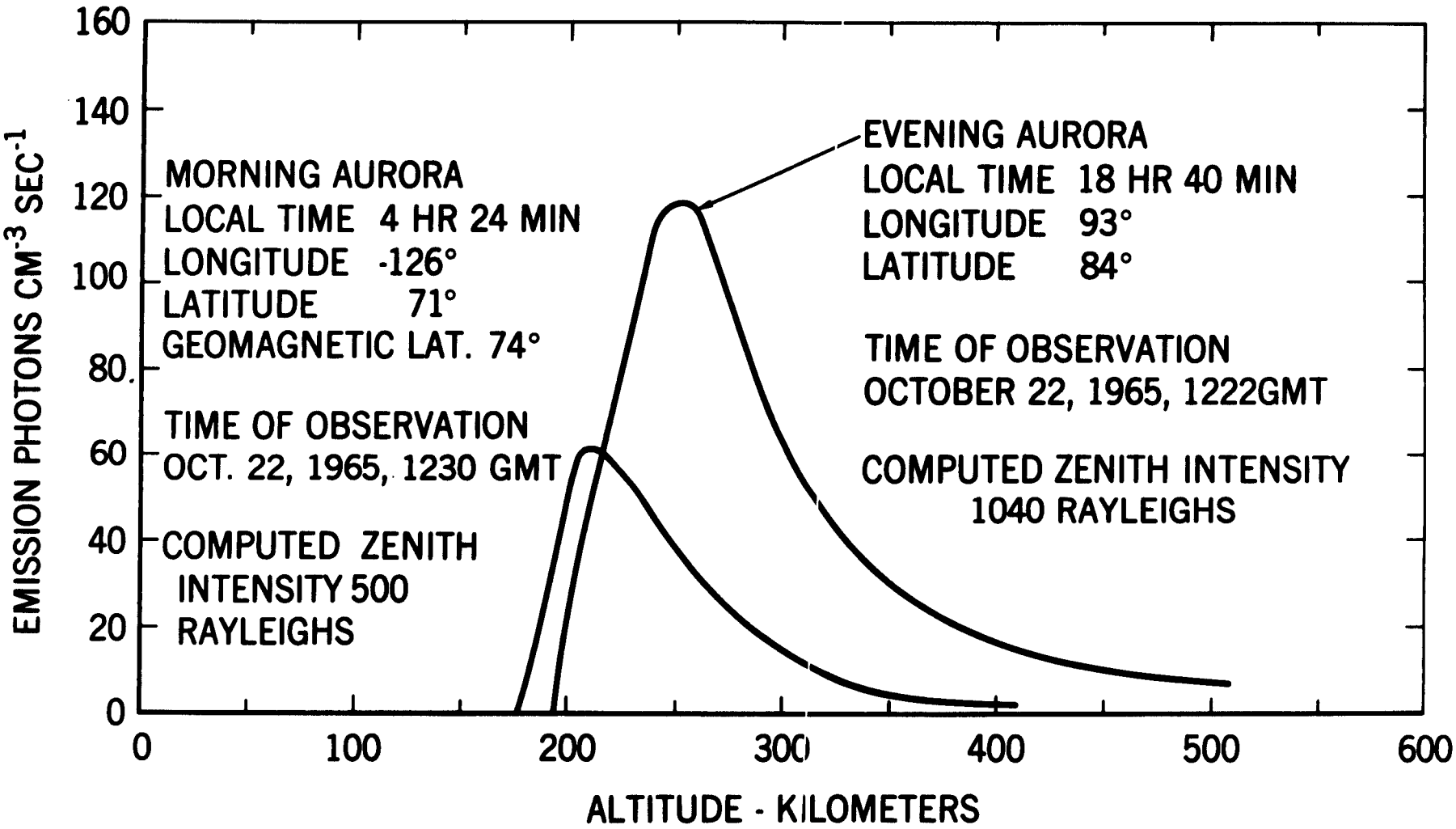

Figure 13. The computed emission profile of aurora using OPEP data only, assuming thin uniform horizontal layers.